J. Biol. Chem. 255, 6234-6237.
Powell, L. W., Alpert, E., Isselbacher, K. J., & Drysdale, J. W. (1975) Br. J. Haematol. 30 47-55.
Richter, G. W (1978) Am. J. Pathol. 91, 363-396.
Russell, S. M., & Harrison, P. M. (1978) Biochem. J. 173, 91-104.
Russell, S. M., Harrison, P. M., & Shinjo, S. (1978) Br. J. Haematol. 38, 296-298.
Stefanini, S., Chiancone, E., & Antonini, E. (1976) FEBS Lett. 69, 90-94.
Wagstaff, M., Worwood, M., & Jacobs, A. (1978a) Br. J. Haematol. 39, 624-625.
Wagstaff, M., Worwood, M., & Jacobs, A. (1978b) Biochem. J. 173, 969-977.

Subunit Structure and Physical Properties of the Hemocyanin of the Giant Isopod *Bathynomus giganteus*†

K. E. Van Holde* and Michael Brenowitz‡

ABSTRACT: The hemocyanin of the deep sea dwelling isopod *Bathynomus giganteus* has been isolated. From the determination of the sedimentation coefficient ($s^0_{20,w}$ = 16.6 S) and the diffusion coefficient ($D_{20,w}$ = 3.1 × 10^{-7} cm^2/s at 1.12 mg/mL), a molecular weight of 4.7 × 10^5 was calculated. The 16S molecule is the largest aggregate observed even under conditions of temperature, pressure, and concentration simulating in vivo conditions. The dissociation of the 16S molecule to 6S monomers is dependent on pH and divalent cation concentration. The sedimentation coefficient and calculated molecular weight are consistent with a hexameric native molecule composed of six monomers of molecular weight about 70 000–80 000, as has been observed for other hemocyanins. The constituent subunits are heterogeneous on both sodium dodecyl sulfate (two bands, 70 200 and 71 800 molecular weight) and nondenaturing alkaline electrophoresis (three bands). In the presence of 10 mM $CaCl_2$, the hexamer is stable to above pH 9.0. Upon dialysis vs. buffer containing 10 mM ethylenediaminetetraacetate, the hemocyanins begin to dissociate into monomers at pH 8.0. The pH-dependent hexamer–monomer dissociation is slowly equilibrating and completely reversible and obeys the law of mass action. The reaction can be described by a cooperative mechanism with one proton binding per monomer. The oxygen binding properties of the hexamer hemocyanin are characterized by a large positive Bohr effect (P_{50}'s at pH 9 and 7 are 5.6 and 57.5, respectively) and moderate cooperativity (n_H = 1.8–3.0). Divalent cations do not appreciably affect either the oxygen affinity or the cooperativity of the hexamer. Complete dissociation to monomers yields noncooperative binding, as expected. The oxygen binding curves of partial dissociation mixtures are well represented by the weighted sum of the curves for "pure monomer" and "pure hexamer" conditions. Comparison of the oxygen binding properties of this deep sea animal with coastal and intertidal species suggests that physiological requirements are more important than phylogenetic relationships in determining the properties of the oxygen-transport protein of a particular species.

The subunit structure, equilibria, and oxygen binding of hemocyanin have been the subject of numerous studies [for reviews, see Van Holde & Van Bruggen (1971), Antonini & Chiancone (1977), and Bonaventura et al. (1977)]. Recent interest in these proteins has centered mainly around two topics: the assembly of the subunits into the native oligomers and the homotropic and heterotropic interactions which influence oxygen binding. Arthropod hemocyanins are assemblies of ca. 70 000-dalton polypeptides organized into hexameric building blocks. In most cases, larger polymers are formed. The aggregation state to which the subunits assemble is species dependent with native molecules ranging in size from a single hexamer (in *Panulirus* and *Penaeus* hemocyanins for example) to an eight-hexamer, 48-subunit molecule found in *Limulus* hemocyanin (Kuiper et al., 1975; Brouwer et al., 1978; Johnson & Yphantis, 1978). The hexamers, dodecamers, etc. isolated from different species have similar morphology when examined in the electron microscope. This observation supports the application of information gained from studies of a single species to the properties of arthropod hemocyanins in general.

The stability of the oligomer is usually dependent on a combination of factors including pH, ionic strength, divalent cation concentration, and oxygen binding. Different conditions are often required to stabilize each level of aggregation [for examples, see Miller & Van Holde (1974), Kuiper et al. (1975), and Brenowitz et al. (1980)]. It is thus necessary to study each association–dissociation reaction separately to understand its importance to the assembly of the whole molecule. An additional complication in studying assembly is heterogeneity of the constituent polypeptides (see reviews). Differences in the roles of a particular subunit in assembly have been demonstrated for hemocyanins from a number of arthropod species (Jeffrey et al., 1978; Lamy et al., 1977; Bijlholt et al., 1979). For example, the apparent role of the dimeric "linker" subunits which have been found in some hemocyanins is to bridge across the two hexamers stabilizing a dodecamer. This explains the observation that hexamers

† From the Marine Biological Laboratory, Woods Hole, Massachusetts 02543. *Received January 16, 1981.* This research was supported in part by Grant GM 00265 to the Marine Biological Laboratory and in part by National Institutes of Health Grant 15460 and Office of Naval Research Grant N 00014-79-C-0178 to Drs. Celia and Joseph Bonaventura, Marine Biomedical Center, Duke University Marine Laboratory.

* Address correspondence to this author at the Department of Biochemistry and Biophysics, Oregon State University, Corvallis, OR 97331.

‡ Present address: Department of Biochemistry, Duke University Marine Laboratory, Beaufort, NC 28516.

0006-2960/81/0420-5232$01.25/0

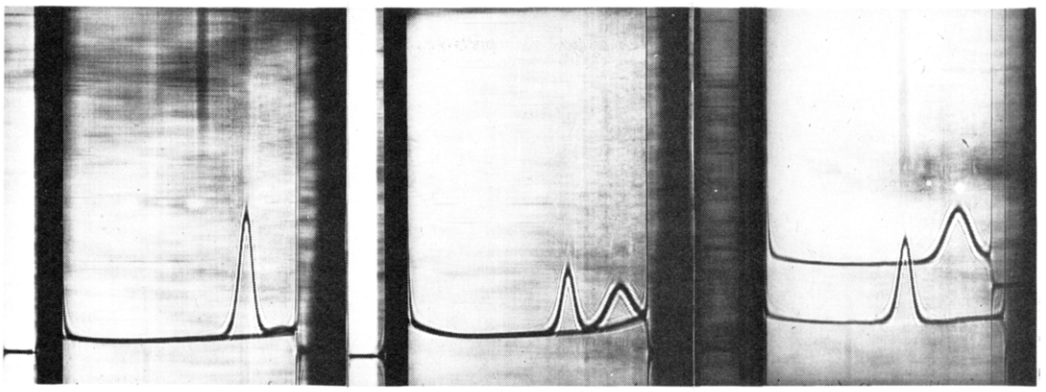

FIGURE 1: Schlieren photographs of (left panel) hemolymph diluted 1:4 in filtered seawater, (center panel) pure hemocyanin dialyzed vs. pH 8.90 Tris–EDTA buffer at room temperature, and (right panel) hemocyanin dissociated by dialysis against pH 9.45 glycine–EDTA (top curve) and hemocyanin that had been dissociated at pH 9.8 after dialysis back to pH 7.85 (bottom curve). Note that no 6S material remains.

have not been detected in the partial dissociation products of some of the larger hemocyanins. Because of such complications, it is very difficult to study the fundamental step, the monomer–hexamer reaction, in the majority of hemocyanins which are capable of further association.

Our laboratories have had a continuing interest in the interactions and assembly of arthropod hemocyanins, and when the opportunity recently arose to investigate the hemocyanin of a quite unusual arthropod, the giant isopod *Bathynomus giganteus*, we felt a preliminary characterization was in order. A short abstract describing these experiments has been published (Van Holde & Brenowitz, 1980). In the course of this work, we found that the hemocyanin from this creature has properties useful for a more general investigation of the interactions involved in the assembly of hemocyanins. In particular, the hexameric native molecule, under certain conditions, is in equilibrium with monomers. The simple equilibrium and limited subunit heterogeneity of this hemocyanin make this a promising system for a more detailed analysis of the monomer–hexamer aggregation of hemocyanins than has been possible to date.

An analysis of this hemocyanin is also of interest from a more biological point of view. The isopod *Bathynomus* dwells in the Gulf of Mexico off the edge of the continental shelf in a habitat of constant temperature, consistently high oxygen availability, and high pressure. By contrast, the isopod *Ligia exotica*, studied by Terwilliger et al. (1979), lives in the rigorous and fluctuating environment of the high intertidal zone with extreme variation in temperature and oxygen availability. Thus, a comparison of the oxygen binding characteristics of the two species may help to evaluate the role that the respiratory protein plays in allowing an organism to adapt to a new environment.

Experimental Procedures

Collection and Purification of the Hemocyanin. The animals had been collected by dredging at about 250 fathoms in the Gulf of Mexico. They were maintained in chilled (~10 °C), circulating seawater and were active at the time samples were taken. Hemolymph was obtained by cutting through several legs and allowing the fluid to drain into test tubes; it immediately formed a clear gelantinous clot. The clot was squeezed through cheesecloth, and the fluid was then centrifuged at low speed for 5 min. As will be shown below, the principal solute component at this point is hemocyanin. Separation from low molecular weight material was effected in two ways: either (a) by pelleting by centrifugation at 65000 rpm for 1 h in a Beckman 65 rotor or (b) by gel filtration on Bio-Gel A5M, using 0.1 ionic strength tris(hydroxymethyl)-aminomethane (Tris)[1] buffer (pH 7.37) containing 10 mM $CaCl_2$ and 10 mM $MgCl_2$.

Buffer Solutions. All experiments were performed in 0.1 ionic strength Tris or glycine buffers, prepared according to the recipes of Long (1961). In some cases, 10 mM $CaCl_2$ and $MgCl_2$ were added; in other cases, 10 mM EDTA was present.

Sedimentation Experiments. Sedimentation studies were carried out in a Beckman Model E ultracentrifuge, equipped with an RTIC unit. Schlieren optics were employed for all sedimentation velocity experiments; the diffusion experiment utilized Rayleigh optics. Most of the sedimentation velocity experiments were carried out at 23–24 °C; a few were at 6–7 °C. Plates were measured on a Nikon comparator, and the relative areas of peaks were determined from the weights of cut-out tracings of the boundary pattern on the comparator screen. Radial dilution corrections were applied in each case, and where appropriate, approximate correction for the Johnston-Ogston effect was made (Schachman, 1959). All sedimentation coefficients were corrected to standard conditions in the usual way.

Electrophoresis. All the electrophoretic analyses were performed on 18-cm-long polyacrylamide slabs. The gels were stained with 1% Coomassie blue G-250 solutions in 25% trichloroacetic acid and destained in methanol–acetic acid–water solution. Electrophoresis of subunits at pH 8.9 was as described by Davis (1964) on 10% acrylamide gels with 0.1 mM EDTA added to the buffers. Samples of hemocyanin were dialyzed vs. pH 9.5 glycine, $I = 0.1$, and 10 mM EDTA buffer overnight prior to electrophoresis. $NaDodSO_4$ electrophoresis was as described by Laemmli (1970) on 6% gels. Electrophoresis of the 16S molecule was performed with the pH 7.8 system of Jeffrey et al. (1976) utilizing 4% gels. Samples were dialyzed against the pH 7.8 buffer overnight prior to electrophoresis.

Oxygen Equilibria. Oxygen binding was measured in tonometers by the method of Riggs & Wolbach (1956). Fractional saturation was determined from the absorbance at 340 nm. The same buffer solutions and protein concentration (ca. 4 mg/mL) were used as for the sedimentation velocity experiments. Samples were dialyzed at room temperature overnight.

Results

Characterization of the Hemocyanin Component. The major protein in the hemolymph of this organism is a single hemocyanin component. This is illustrated in the left panel of Figure 1, which shows the Schlieren pattern obtained when

[1] Abbreviations used: Tris, tris(hydroxymethyl)aminomethane; EDTA, ethylenediaminetetraacetate; $NaDodSO_4$, sodium dodecyl sulfate.

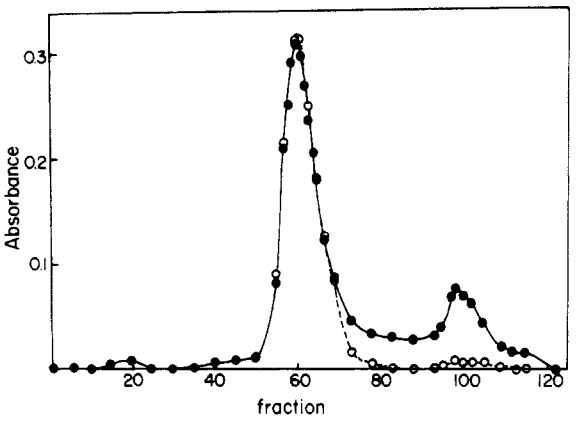

FIGURE 2: Purification of the hemocyanin by gel filtration on Bio-Gel A5m. (●) Absorbance at 280 nm (2-mm path length); (○) absorbance at 340 nm (10-mm path length).

the hemolymph (after removal of the clot) is diluted 1:4 in filtered seawater. The major component has a sedimentation coefficient under these conditions of about 15 S. From the area under the boundary, we estimate the concentration of this component in hemolymph to be about 30 mg/mL. The gel filtration profile shown in Figure 2 also shows that the component which absorbs strongly at 340 nm constitutes the larger part of the hemolymph protein. A smaller amount of material which absorbs at 280 nm (but not at 340 nm) runs more slowly through the column.

Under no conditions have we observed larger hemocyanin components than that shown in the left panel of Figure 1, nor do we believe that such exist in vivo. We have sedimented whole hemolymph, with an overlay of 0.4 cm of mineral oil to simulate the pressure under which the organism normally lives. At 42040 rpm, the pressure of the meniscus corresponded to that of approximately 1700 ft of seawater. The experiment was done at 10 °C to further simulate the in vivo conditions. Almost all of the material sedimented at $s_{20,w}$ = 11.3 S. This value has not been corrected for the viscosity and density of the hemolymph nor the effect of hemocyanin concentration. Applying an approximate correction for the concentration dependence of the sedimentation coefficient, based on the estimated hemolymph concentration, we obtain $s^0_{20,w}$ = 16 S. Clearly, this is the same component we observed in the left panel of Figure 1.

At high pH, in the absence of divalent cations (i.e., in buffers containing 10 mM EDTA), the hemocyanin completely dissociates into a more slowly sedimenting component. The progress of this dissociation is illustrated in Figure 3. We shall describe this process in more detail below but shall first characterize the two components. $s_{20,w}$ vs. C curves for the native hemocyanin and the dissociation product were determined. Concentrations were determined either from the absorbance at 340 nm or from the areas under Schlieren peaks. Both were calibrated from a synthetic boundary cell experiment with Rayleigh optics, with the assumption that each Rayleigh fringe corresponds to 0.2324 mg/mL (Nickerson & Van Holde, 1971). Values of 1.28 and 0.276 [(mg/mL) cm]$^{-1}$ were thus obtained for extinction coefficients at 280 and 340 nm, respectively. The $s^0_{20,w}$ values for the native and dissociated hemocyanin are found to be 16.6 and 5.55 S, respectively. These correspond closely to values obtained for a number of other arthropod hemocyanins (Van Holde & Van Bruggen, 1971). We shall henceforth refer to these as the "16S" and "6S" components.

The synthetic boundary experiment, carried out at pH 8.22 in Tris buffer with 10 mM Ca^{2+} and Mg^{2+}, was also utilized

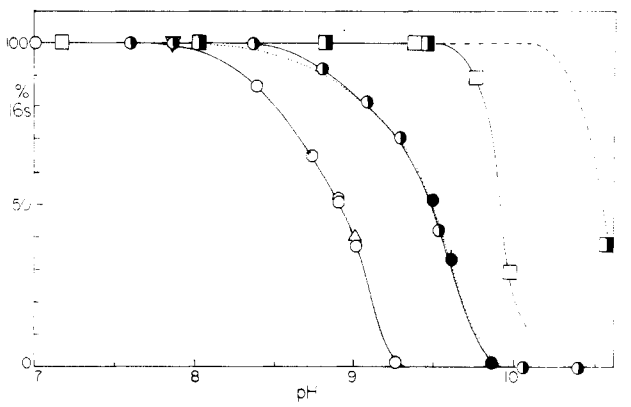

FIGURE 3: Dissociation–association equilibrium of *Bathynomus* hemocyanin as a function of pH. Squares are with $CaCl_2$ and $MgCl_2$ present, and circles are with EDTA present. Solid symbols are for solutions which were equilibrated and run at 6–7 °C. Half-filled symbols are for samples equilibrated at 6–7 °C and run immediately at 23–24 °C. Open symbols are experiments which were both equilibrated and run at 23–24 °C. The tagged circle is for an experiment first equilibrated and run at 6 °C and then reequilibrated and run at 24 °C, open triangle. The inverted triangle is for samples which were partially (pH 8.21) or wholly (pH 9.8) dissociated and then dialyzed back to pH 7.85 for reassociation. The dashed lines indicate likely curves in regions of insufficient data. The dotted line is the theoretical line for a cooperative monomer–hexamer equilibrium (see text).

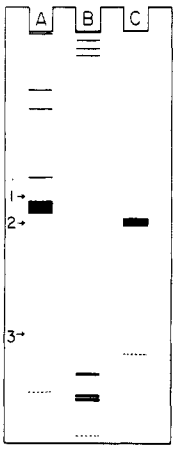

FIGURE 4: Electrophoresis gels of (A) $NaDodSO_4$, (B) pH 8.9 subunit, and (C) pH 7.8 16S molecule. The arrows next to column A indicate the mobility of the standards: (1) transferrin, 77000; (2) BSA, 66000; (3) ovalbumin, 43000.

to estimate the diffusion coefficient, and hence the molecular weight of the 16S component. We obtain $D_{20,w} = 3.1 \times 10^{-7}$ cm^2/s at 1.12 mg/mL. From this value, the above value of $s^0_{20,w}$, and the assumption that $\bar{v} = 0.725$ as for other arthropod hemocyanins (Carpenter & Van Holde, 1973; Roxby et al., 1974), we obtain a molecular weight of 4.7×10^5. This must be regarded as only approximate, since only a single value of $D_{20,w}$, not extrapolated to zero concentration, has been employed.

The molecular weight for the 16S component can also be estimated on the basis of its sedimentation coefficient and the behavior of other globular proteins. A value of about 4.5×10^5 daltons is obtained. The assumption that this hemocyanin component is in fact globular is supported by the hydrodynamic behavior of similar 16S hemocyanin components, as well as electron microscopy (Van Holde & Van Bruggen, 1971). Since we know nothing about the conformation of the 6S component, we cannot use this technique in this case. Analysis of the dissociated subunits by $NaDodSO_4$ gel electrophoresis (Figure 4A) yields evidence for two polypeptide chains, with

almost identical molecular weights of 71 800 and 70 200 (values are the average of two determinations). From these results, we conclude that the 16S component is a hexamer of 6S polypeptide chains, as commonly observed for arthropod hemocyanins.

Electrophoresis. Alkaline electrophoresis of the undenatured monomers revealed three bands, a doublet with components differing slightly in mobility and a single lower mobility band (Figure 4B). The components of the doublet stained about equally and more intensely than the slower band. A small amount of high molecular weight material, probably undissociated or partially dissociated hexamers, was also present. This is probably due to reassembly of the protein in the pH 6.8 stacking gel used in this protocol, despite the presence of EDTA in the buffers. As mentioned in the previous section, a doublet was also observed on $NaDodSO_4$ gels (Figure 4A). Again, a small amount of high molecular weight material was present. The separation of the monomer bands was insufficient to quantitatively determine the relative amounts of the bands. Qualitatively, the two $NaDodSO_4$ bands appeared in roughly equal proportions.

Electrophoresis of the hexamer yields only a single band at pH 7.8 (Figure 4C). Using this protocol, Jeffrey et al. (1976) were able to resolve three hexamer isozymes for *Cherax destructor* hemocyanin. Thus, even though a continuous buffer protocol, such as the one used here, does not have particularly high resolution, we believe that only a single hexamer is present in *Bathynomus* hemocyanin.

Analysis of the Monomer–Hexamer Equilibrium. In the presence of 10 mM Ca^{2+} and 10 mM Mg^{2+}, the 16S component is stable to quite high pH values (Figure 3). However, when these ions are removed by dialysis against 10 mM EDTA at alkaline pH, dissociation to monomer occurs (Figure 3). All points on these curves were obtained from sedimentation patterns of the kind shown in the center and right panels of Figure 1. Boundaries were well resolved, and the sedimentation coefficient of both components remained virtually unchanged, despite the large changes in proportions. These facts lead us to believe that the system is not in rapid equilibrium. Each point was determined on a solution which had been equilibrated by dialysis either at room temperature or at 6 °C for at least 18 h. The pH range at which dissociation occurs depends on the temperature of dialysis (Figure 3). As Figure 3 shows, data on solutions equilibrated at 6 °C and immediately run at room temperature lie on the same curve as data from solutions equilibrated at 6 °C and run at 6 °C. Therefore, we have plotted all data vs. the pH of the buffer at the dialysis temperature. All data in Figure 3 have been corrected for radial dilution but have not been corrected for the Johnston-Ogston effect which was judged to be barely significant at the concentration (ca. 4 mg/mL) used in these experiments (see below).

To be assured of the validity of any detailed analysis of these dissociation curves, we must first show that the reaction is in fact reversible and that the points represent equilibrium mixtures. Such is often not the case in hemocyanin association–dissociation processes [see Kuiper et al. (1975) and Terwilliger et al. (1979) for examples involving monomer–hexamer reactions of arthropod hemocyanins, and Van Holde & Van Bruggen (1971) for a more general discussion]. We have therefore applied three separate and independent tests for an equilibrating system:

(*a*) *Reversibility.* We find that after dissociation of the hemocyanin by an increase in pH, lowering the pH can lead to complete reassociation. This has been demonstrated both with partial dissociation at pH 9.08 and after complete dissociation at pH 9.8 (see Figure 3 and right panel of Figure 1). It is evidently possible to quantitatively reform 16S particles from the dissociated monomers, for Figure 1 (right panel, bottom curve) reveals no residual 6S material nor did any material precipitate during dialysis. Actual measurement, corrected for radial dilution, yields less than 1% change in total area.

(*b*) *Separation Experiment.* A concentrated (ca. 8 mg/mL) sample of partially dissociated hemocyanin at pH 9.01 (about 60% 16 S) was centrifuged until the fast boundary was moved past the partition position in a moving partition cell. After the run was decelerated, the supernatant (6S) material was removed and allowed to reequilibrate for 20 h. It was then analzyed again and compared with a sample of the original solution which had been diluted approximately 1:1. The comparison was done in this way, since we had observed (see below) that the mass action law is at least approximately followed by this system and the supernatant material from the partition cell was only about half as concentrated as the original solution. The reequilibrated 6S material was now found to contain 41% of the 16S component; the comparison solution had 37% of the 16S material. Thus, the approximate amount of hexamer expected has been formed. Furthermore, the fact that separation could be obtained at all reaffirms that equilibrium is only slowly attained.

(*c*) *Test of the Mass Action Law.* A series of dilutions of the stock hemocyanin solution was dialyzed for 24 h at 6 °C against Tris buffer, pH 8.80, containing 10 mM EDTA. The solutions were analyzed by sedimentation velocity, and the relative areas of the peaks were measured and corrected for radial dilution. Corrections for the Johnston-Ogston effect were also applied, using the method described by Schachman (1959). This correction was significant only at the highest concentration. The data were analyzed in the following way: If we have a monomer–hexamer equilibrium

$$6M \rightleftarrows H \tag{1}$$

then we may write an equilibrium constant

$$K = C_H/C_M{}^6 \tag{2}$$

where C_H and C_M represent weight concentrations of hexamer and monomer, respectively. With C_0 as the total weight concentration and α as the weight fraction of hexamer, this becomes

$$K = \frac{\alpha C_0}{(1-\alpha)^6 C_0{}^6} = \left(\frac{1}{C_0{}^5}\right)\left(\frac{\alpha}{(1-\alpha)^6}\right) \tag{3}$$

or

$$\log \frac{\alpha}{(1-\alpha)^6} = 5 \log C_0 + \log K \tag{4}$$

Figure 5 shows the graph of $\log [\alpha/(1-\alpha)^6]$ vs. $\log C_0$. While not all four points fall on the line with the theoretical slope of 5.0, there is clearly much dissociation upon dilution, and the data can be said to approximately demonstrate the theoretically expected behavior. It should be pointed out that this is a very sensitive test, since all errors in α (especially as $\alpha \rightarrow 1$) are greatly magnified in $(1-\alpha)^6$. The apparent deviation at high C_0 could thus result from a small error, neglected nonideality, or inadequacy of the Johnston-Ogston correction.

pH Dependence of the Equilibrium. We believe that the above results (see parts a–c above) show that the system can be regarded, to a first approximation at least, as a slowly equilibrating monomer–hexamer system. We therefore feel

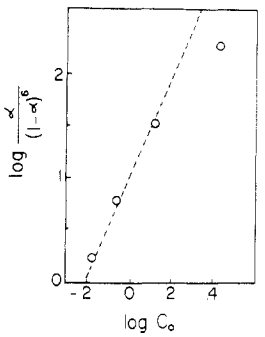

FIGURE 5: Test of the mass action law; dissociation, expressed as log $[\alpha/(1-\alpha)^6]$ vs. log C_0 (arbitrary units). The dashed line has the theoretically expected slope of 5.0.

justified in proceeding to an analysis of the pH dependence of this equilibrium.

It is evident from Figure 3 that an uptake of protons must accompany the association of monomers to form hexamers. We first attempted to analyze the reaction with the following scheme, making the assumption that only monomer protonated at a given site could enter into the equilibrium. Protonated and unprotonated monomers are assumed to be in equilibrium.

$$M + H^+ \rightleftarrows MH^+ \qquad K_a = [M][H^+]/[MH^+] \quad (5)$$

$$6(MH^+) \rightleftarrows P \qquad K = [P]/[MH^+]^6 \quad (6)$$

However, this scheme is not successful; no real value of pK_a could be obtained which would fit the data. Therefore, we have tried a cooperative mechanism:

$$6M + nH^+ \rightleftarrows P \qquad K = [P]/([M]^6[H^+]^n) \quad (7)$$

In essence, this scheme assumes that there is no appreciable concentration of *free* monomer protonated at the site(s) involved in the association reaction. It is equivalent to assuming that virtually all protonated monomers are incorporated into polymers.

Equation 7 can be rewritten in terms of weight concentration and α, the weight fraction of hexamer:

$$K = \left(\frac{M_r^5}{6C_0^5}\right)\left(\frac{\alpha}{(1-\alpha)^6}\right)\left(\frac{1}{[H^+]^n}\right) \quad (8)$$

or

$$\log \frac{\alpha}{(1-\alpha)^6} = A + n \log [H^+] \quad (9)$$

$$\log \frac{\alpha}{(1-\alpha)^6} = A - n\,(pH) \quad (10)$$

where

$$A = \log K + \log \frac{6C_0^5}{M_r^5} \quad (11)$$

M_r being the molecular weight of the monomer.

Thus, a graph of log $[\alpha/(1-\alpha)^6]$ vs. pH should be a straight line with a slope = $-n$. Such graphs for data at 23–24 and 6–7 °C are shown in Figure 6. Clearly, the fitting is quite good. The slope n is determined to be 7.1; we feel that this is so close to 6 that it indicates that one proton is acquired by each monomer as it enters a hexamer. Accordingly, we have used the corresponding equation with $n = 6$ to generate the dotted line in Figure 3. The agreement is all that one might expect, considering the uncertainty in the assumptions and the experimental data. Note that the theory predicts quite nicely the asymmetric form of the dissociation curve. We conclude, therefore, that protonation of one critical group in each monomer is essential to association. Unfortunately, the theory does not allow a determination of the pK_a of this group. Clearly, it must be in the vicinity of pH 9 at room temperature and shift upward about 0.6 pH unit when the temperature is decreased to 6 °C. This suggests the involvement of an amino group, presumably either the N terminal or a lysine side chain.

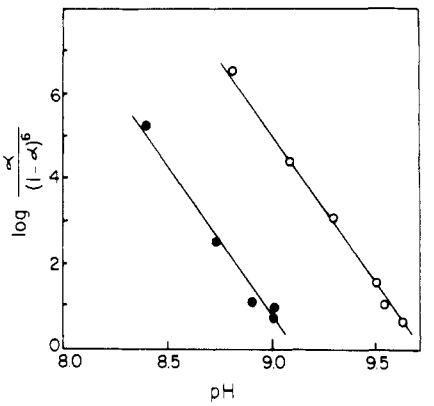

FIGURE 6: Test of the "cooperative" mode of the H^+-mediated association. (○) After equilibration at 6–7 °C; (●) after equilibration at 23–24 °C. Both lines have a slope of 7.1.

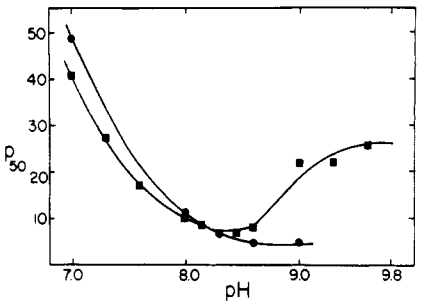

FIGURE 7: Dependence of oxygen affinity (P_{50}) on pH with 10 mM $CaCl_2$ (●) or 10 mM EDTA present (■). P_{50} is in millimeters of mercury.

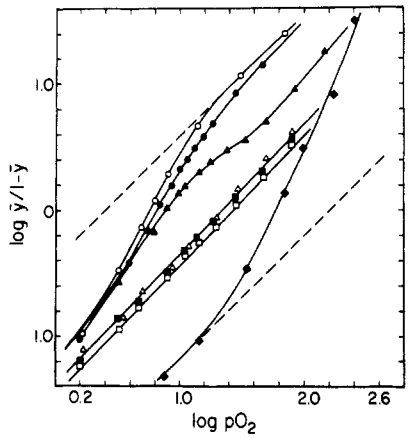

FIGURE 8: Hill plots of oxygen binding experiments: (○) pH 9.0, 10 mM $CaCl_2$; (●) pH 8.45, 10 mM EDTA; (▲) pH 8.8, 10 mM EDTA; (△, ■, □) pH 9.0, 9.3, and 9.6, 10 mM EDTA; (♦) pH 7.0, 10 mM $CaCl_2$. The dashed lines estimate the high- and low-affinity asymptotes and have a slope of unity.

Oxygen Equilibria. Two sets of oxygen binding curves were measured, one in the presence of 10 mM $CaCl_2$, the other in the presence of 10 mM EDTA. The pH dependence of the oxygen affinity is shown in Figure 7. In the presence of calcium, a large positive Bohr effect is observed between pH 7.0 and 9.0. The Hill plots are a series of sigmoidal curves lying between the curves from pH 9 and 7 shown in Figure 8. Sedimentation velocity experiments have shown the 16S

molecule to be stable in the presence of calcium within this entire pH range (Figure 3). In the absence of calcium (10 mM EDTA), a very similar Bohr effect is evident up to pH 8.4; the Hill plots in this range resemble those obtained in the presence of Ca^{2+} (data not shown). Dissociation begins above pH 8; at pH 8.4, sedimentation studies show about 20% monomer (Figure 3). Complete dissociation to monomers, at pH 9.3 and above in the absence of calcium, yields noncooperative Hill plots exhibiting lower affinity than that of the aggregated protein in the alkaline pH range (Figure 8; compare pH 9.0, 10 mM $CaCl_2$, and pH 9.0, 10 mM EDTA, curves). Under all conditions where oxygen binding was examined, the curves fit between the limiting lines of $n = 1$ defining the allosteric range for this system (broken lines in Figure 8). Extrapolation of these limits gives P_{50} values of 2.5 and 158.4 mmHg, respectively, for the limiting values.

The effect of the pH-dependent monomer–hexamer equilibrium is evident in Hill plots of the oxygen binding data between pH 8.45 and 9.6 in the absence of calcium (Figure 8). Since the equilibrium is slow, we believe no changes in the amount of monomer and hexamer occur during the binding experiments. Then we should be able to predict the form of the binding curves in the transition region from the proportion of monomer and hexamer shown in Figure 3. The pH 8.6, 10 mM $CaCl_2$ curve and the pH 9.3, 10 mM EDTA curves were used as the binding curves for the "pure hexamer" and "pure monomer", respectively. The hexamer shows little change in affinity in the range pH 8.2–9.0 (Figure 7). That the monomers do not show a significant change in P_{50} between pH 9.0 and 9.6 is at least partial justification for using the pH 9.3 monomer curve for the calculations at lower pH (Figure 7). The addition of the two "pure species curves" utilized the following equation:

$$Y_C = Y_H(\alpha) + Y_M(1 - \alpha) \qquad (12)$$

where Y_C is the fractional saturation of the composite curve, Y_H is for "pure" hexamer, Y_M is for "pure" monomer, α = fraction of hexamer in the mixture, and $1 - \alpha$ = fraction of monomer in the mixture.

This takes into account both the relative proportion of the components and the differences in contribution of the two curves (due to differing affinity and cooperativity) at different partial pressures. The calculated curves for pH 8.45 and 8.8 are shown by the dashed lines in Figure 9. The symbols are the measured data points. At pH 8.45, the best fit was achieved with 87% hexamer and at pH 8.8 with 60% hexamer. The fit of the calculated curves is good except at the higher pO_2 values at pH 8.8. The expected values from Figure 3 at these pHs are 83% and 60% hexamer, respectively, in very good agreement with the values calculated by the curve fitting.

Cooperativity is not dependent on the presence of divalent cations. Hill coefficients for the 16S hexamer (from pH 7 to 8.45) varied from 3 to 1.8 with either 10 mM $CaCl_2$ or 10 mM EDTA present in solution. At those pH values where the hexamer is stable, the chelation of calcium by EDTA caused a slight increase in oxygen affinity (Figure 7). Increasing the ionic strength with 2 M NaCl increased the oxygen affinity at pH 7.0 from 47.5 to 25.5 (10 mM $CaCl_2$) and from 41.0 to 25.5 (10 mM EDTA).

Discussion

Bathynomus hemocyanin is a particularly clear example of an arthropod hemocyanin incapable of association beyond the hexameric state. Hexamers have been reported as the sole component of the hemolymph of a number of diverse arthropod species including some crayfish (Moore et al., 1968; Kuiper et al., 1975; Markl et al., 1979), some shrimp and hermit crabs (Ghiretti et al., 1973), and a number of isopods (Bethet et al., 1964). However, in only a few cases (Moore et al., 1968; Kuiper et al., 1975) has it been demonstrated, as here, that the hemocyanin is incapable of association beyond the hexameric state under a wide variety of conditions. It seems likely that such hemocyanins lack the "linker" subunits that appear to be involved in higher polymerization [see Jeffrey et al. (1976), Markl et al. (1979), and Bijlholt et al. (1979)]. However, it must not be thought that a hexameric hemocyanin is a general feature of isopod hemocyanins. A careful study by Terwilliger et al. (1979) has shown that the hemocyanin of the isopod *Ligia exotica* exists in the hemolymph primarily as a 24S dodecamer. The existence of a well-behaved, if slowly attained, equilibrium between hexamers and monomers of *Bathynomus* hemocyanin is in clear contrast to the behavior of the hemocyanin of the closely related *Ligia*. In this case, both hexamers and dodecamers were observed in the hemolymph, and dissociation of hexamers to monomers was only partial at the highest pHs studied (10.5). Furthermore, the separated monomers did not reequilibrate. Their results indicate that the dissociated hexamers at pH 9.5 are of a different subunit composition than those which remain intact. Yet, Terwilliger et al. were not able to demonstrate electrophoretic heterogeneity of hexamers.

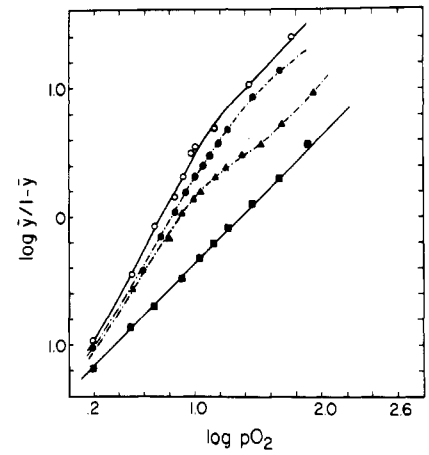

FIGURE 9: Calculation of the oxygen binding curves of the monomer–hexamer equilibrium from "pure" monomer and hexamer curves (see text): (○) pH 8.6, 10 mM $CaCl_2$; (●) pH 8.45, 10 mM EDTA; (▲) pH 8.8, 10 mM EDTA; (■) pH 9.3, 10 mM EDTA. Broken lines indicate the calculated curves in situations where mixtures of monomers and hexamer are present.

We observed a similar puzzling aspect of our results. From the electrophoretic analysis, it is clear that *Bathynomus* subunits are heterogeneous. In fact, the subunit composition of *Bathynomus* hemocyanin is similar to that determined for other hexameric hemocyanins. On $NaDodSO_4$ gels, two bands are observed for *Bathynomus* and *Penaeus* hemocyanins, while three bands are apparent on gels of *Ligia* and *Panulirus* hemocyanins (Brouwer et al., 1978; Terwilliger et al., 1979; Kuiper et al., 1975). However, only in the case of *Bathynomus* has subunit heterogeneity been demonstrated by using a nondenaturing gel system. One might expect that such a clear subunit heterogeneity would imply a heterogeneity in the dissociation equilibrium. That is, there is no a priori reason to expect that all subunit types should exhibit equal free energies of interaction. There appear to be two ways out of this dilemma. First, it is possible that one combination of subunits would be so favored that there is essentially only one kind of hexamer formed, which exhibits only one dissociation–association equilibrium. This is certainly consistent with our ob-

Table I

	Panulirus[a]	*Penaeus*[b]	*Ligia*[c]	*Bathynomus*
P_{50}, 10 mM $CaCl_2$				
pH 7.0	54	54	1.44	57.5
pH 9.0	7	0.55	0.93	5.6
n_H (10 mM $CaCl_2$)	2.0–2.7	2.8–4.0	3.2–4.0	1.8–3.0
$CaCl_2$ required for cooperativity?	no	no	no	no
P_{50}, 0.1 M NaCl		3.3; pH 8.2	400;[d] pH 8.0	47.5; pH 7.0
2.0 M NaCl		0.2	100[d]	25.5
P_{50}, 10 mM $CaCl_2$	24; pH 7.6	10.5; pH 7.8	0.95; pH 8.0	15.8; pH 8.0
no added $CaCl_2$	10	5.6	1.55	12.0

[a] Kuiper et al. (1975). [b] Brouwer et al. (1978). [c] Terwilliger et al. (1979). [d] Oxygen dissociation constants, K (s^{-1}).

servation of only one dissociation–association equilibrium and only a single hexamer component. However, the results of Terwilliger et al. referred to above make us hesitant to attach too much importance to this evidence.

A second possibility resides in the fact that differences in subunits, detected by electrophoresis, may not always be significant indicators of differences in interactions between subunits. That is, electrophoretically distinct subunits may be functionally equivalent. For example, recent studies of *Limulus* hemocyanin subunits (Brenowitz et al., 1981) indicate that not all separable subunits act distinguishably in the assembly of larger structures. A planned immunological study of *Bathynomus* hemocyanin will hopefully clarify this point.

We turn now to consideration of the pH dependence of the equilibrium. Since experiments in which the solution was dialyzed at 6 °C and centrifuged at that temperature gave the same results (e.g., percent 16 S) as experiments in which dialysis at 6 °C was immediately followed by centrifugation at room temperature, we judge that it is the conditions of dialysis which determine the percent dissociation. If we plot the data, as in Figure 3, vs. the pH of the buffer solution at the dialysis temperature, two curves are obtained. These are displaced from one another by almost exactly the pH shift which the Tris or glycine buffer systems exhibit over this same temperature interval. The consequence of this, of course, is that a solution which was dialyzed at 6 °C and then allowed to reequilibrate at room temperature will show little changes in 16S/6S ratios (see Figure 3). We believe that this behavior simply reflects the fact that the protein groups which are titrated when hexamer is formed have essentially the same enthalpy of ionization as do Tris or glycine. This should not be surprising, for amino groups are excellent candidates for the groups titrating in this pH range.

The simple way in which the pH dependence of the association–dissociation equilibrium can be analyzed also suggests a homogeneity in the reaction. If there were substantially different kinds of hexamers that could form, with different structures surrounding the critical proton-bonding groups, one would expect the curves in Figure 3 to be broader. However, it is conceivable that a combination of circumstances could be misleading us here; if there were more than one proton required per monomer, and a heterogeneity in hexamers, the sharpening caused by the former might be exactly balanced by the broadening resulting from the latter. But this appears to be a rather unlikely and unnecessarily complicated explanation, considering the excellence of the agreement of the calculated curves and the experimental data.

The oxygen binding behavior of *Bathynomus* hemocyanin can be analyzed in a quite straightforward manner. As long as the hexameric structure is intact (e.g., up to pH 8 in the absence of divalent cations, and to high pH in their presence), the hemocyanin exhibits cooperative binding with Hill coefficients in the range of 2–3 and a strong positive Bohr effect. Under these conditions, the presence of calcium has relatively little effect; thus, there is little intrinsic effect of calcium on the oxygen binding, as distinguished from the mediation of the association–dissociation equilibrium by divalent cations, which can clearly affect the oxygen binding *indirectly*. Complete dissociation to monomers (as at pHs greater than 9.3 in EDTA yields noncooperative binding as expected. Under conditions where dissociation is only partial, the binding curves can be quite well represented as the weighted sum of curves for monomer and hexamer.

A comparison of the oxygen binding behavior of *Bathynomus* hemocyanin with that of three other hexameric hemocyanins is given in Table I. The habitats of the animals are quite different: *Bathynomus* is a deep-sea dweller, *Panulirus* and *Penaeus* are subtidal, moving between the estuaries and the open sea during their life cycle, and *Ligia* is intertidal. In view of this, the similarities of the oxygen binding behavior are more striking than the differences. In particular, *Panulirus*, *Penaeus*, and *Bathynomus* have nearly identical oxygen affinities, Hill coefficients, and Bohr effects in the physiological range. All are active animals, living in environments of relatively abundant oxygen although *Penaeus* and *Panulirus* may experience hypoxia during their life cycles. With both *Penaeus* and *Bathynomus*, high salt concentration increases oxygen affinity, and with all three, divalent cations decrease affinity somewhat. The exception is *Ligia*. It has a much higher affinity near physiological pH and an almost negligible Bohr effect. These features may be advantageous in the fluctuating and relatively anoxic environment *Ligia* sometimes experiences. Taken together, the data emphasize the great importance of physiological requirements as compared to phylogenetic relationships in determining the properties of an oxygen-transport protein in a particular species.

Acknowledgments

We express our special thanks to Dr. Robert B. Barlow, Jr., of the Marine Biological Laboratory and Dr. George Ruggieri of the Osborn Laboratories at the New York Aquarium for making specimens available to us.

References

Antonini, F., & Chiancone, E. (1977) *Annu. Rev. Biophys. Bioeng. 6*, 239–271.

Bethet, J., Baudhuin, P., & Wibo, M. (1964) *Arch. Int. Physiol. Biochim. 72*, 676–677.

Bijlholt, M., Van Bruggen, E. F. J., & Bonaventura, J. (1979) *Eur. J. Biochem. 95*, 399–405.

Bonaventura, J., Bonaventura, C., & Sullivan, B. (1977) in *Oxygen and Physiological Function* (Jobsis, F., Ed.) Professional Information Library, Dallas, TX.

Brenowitz, M., Van Holde, K. E., Bonaventura, C., & Bonaventura, J. (1980) *Fed. Proc., Fed. Am. Soc. Exp. Biol. 39*, 1768.

Brenowitz, M., Bonaventura, C., Bonaventura, J., & Giananza, E. (1981) *Arch. Biochem. Biophys.* (in press).
Brouwer, M., Bonaventura, C., & Bonaventura, J. (1978) *Biochemistry 17*, 2148–2154.
Carpenter, D. E., & Van Holde, K. E. (1973) *Biochemistry 12*, 2231–2238.
Davis, B. J. (1964) *Ann. N.Y. Acad. Sci. 121*, 404–427.
Ghiretti, F., Ghiretti-Magaldi, A., & Salvato, B. (1973) in *Comparative Physiology* (Bolis, L., Schmidt-Nielsen, K., & Maddrell, S. H. P., Eds.) pp 509–522, North-Holland Publishing Co., Amsterdam.
Jeffrey, P. D., Shaw, D. C., & Treacy, G. B. (1976) *Biochemistry 15*, 5527–5533.
Jeffrey, P. D., Shaw, D. C., & Treacy, G. B. (1978) *Biochemistry 17*, 3078–3083.
Johnson, M., & Yphantis, D. (1978) *Biochemistry 17*, 1448–1455.
Kuiper, H. A., Gaastra, W., Beintema, J. J., Van Bruggen, E. F. J., Schepman, A. M. H., & Drenth, J. (1975) *J. Mol. Biol. 99*, 619–629.
Laemmli, U. K. (1970) *Nature (London) 227*, 680–685.
Lamy, J., Lamy, J., Baglin, M.-C., & Weill, J. (1977) in *Structure and Function of Hemocyanin* (Bannister, J. V., Ed.) Springer-Verlag, Berlin and New York.
Long, C. (1961) *Biochemist's Handbook*, Richard Clay and Co., Ltd., Bungay, Suffolk, England.
Markl, J., Hofer, A., Bauer, G., Markl, A., Kempter, B., Brezinger, M., & Linzen, B. (1979) *J. Comp. Physiol. 133*, 167–175.
Miller, K., & Van Holde, K. E. (1974) *Biochemistry 13*, 1668–1674.
Moore, C. H., Henderson, R. W., & Nickol, L. W. (1968) *Biochemistry 7*, 4078–4085.
Nickerson, K. W., & Van Holde, K. E. (1971) *Comp. Biochem. Physiol. B 39B*, 855–872.
Riggs, A. F., & Wolbach, R. A. (1956) *J. Gen. Physiol. 39*, 585–605.
Roxby, R., Miller, K., Blair, D. P., & Van Holde, K. E. (1974) *Biochemistry 13*, 1662–1668.
Schachman, H. K. (1959) *Ultracentrifugation in Biochemistry*, Academic Press, New York and London.
Terwilliger, N. B., Terwilliger, R. C., Applestein, M., Bonaventura, C., & Bonaventura, J. (1979) *Biochemistry 18*, 102–108.
Van Holde, K. E., & Van Bruggen, E. F. J. (1971) *Biol. Macromol. 5*, 1–53.
Van Holde, K. E., & Brenowitz, M. (1980) *Biol. Bull. (Woods Hole, Mass.) 159*, 478.

Human Brain Calmodulin: Isolation, Characterization, and Sequence of a Half-Molecule Fragment†

William E. Schreiber,‡ Tatsuru Sasagawa, Koiti Titani,§ Roger D. Wade, Dean Malencik,‖ and Edmond H. Fischer*

ABSTRACT: A Ca^{2+}-binding protein from human brain has been purified to homogeneity and identified as residues 72–148 of calmodulin. This half-molecule fragment (CaM_{72-148}) contains 11 of calmodulin's 15 basic amino acids (including one trimethyllysine) and demonstrates a higher isoelectric point. Both tyrosines and three of eight phenylalanine residues also occur in the fragment, giving rise to a somewhat different absorption spectrum. Though it contains two of calmodulin's Ca^{2+}-binding sites, CaM_{72-148} binds only one Ca^{2+} per molecule with a dissociation constant of 17 μM. No biological activity, as judged by its inability to activate cyclic nucleotide phosphodiesterase, is observed. The sequence of amino acids is identical with that of residues 72–148 of bovine brain calmodulin [Kasai, H., Kato, Y., Isobe, T., Kawasaki, H., & Okuyama, T. (1980) *Biomed. Res. 1*, 248–264]. CaM_{72-148} is thought to arise through proteolysis, and its implications for the structure and physiological role of calmodulin are discussed.

Calmodulin is a low molecular weight, heat-stable, acidic protein that activates a variety of enzyme systems upon binding calcium [for a review, see Cheung (1980)]. It has been isolated from many species, both animal and plant, and shows a high degree of conservation of biological and physical properties. The primary structure of calmodulin from bovine brain has been completely determined (Watterson et al., 1980; Kasai et al., 1980), and partial sequences exist for bovine uterus (Grand & Perry, 1978) and rat testis (Dedman et al., 1978).

During the purification of calmodulin from human brain, another Ca^{2+}-binding protein of low molecular weight was observed. We have purified this protein to homogeneity and identified it as a fragment of calmodulin, comprising residues 72–148. The physicochemical properties of the fragment, which we call CaM_{72-148},[1] are similar to those of the parent molecule. Since calmodulin has been well characterized from

† From the Department of Biochemistry, University of Washington, Seattle, Washington 98195. *Received March 6, 1981.* This work was supported by grants from the National Institutes of Health (AM 07902, GM 15731, and GM 27335), the National Science Foundation (PCM 7516260), and the Muscular Dystrophy Association.

‡ Recipient of a postdoctoral fellowship from the Muscular Dystrophy Association.
§ Investigator of the Howard Hughes Medical Institute.
‖ Present address: Department of Biochemistry and Biophysics, Oregon State University, Corvallis, OR 97331.

[1] Abbreviations used: CaM_{72-148}, residues 72–148 of calmodulin; CaM_{1-71}, residues 1–71 of calmodulin; Hepes, *N*-2-(hydroxyethyl)-piperazine-*N'*-2-ethanesulfonic acid; HPLC, high-performance liquid chromatography; $NaDodSO_4$, sodium dodecyl sulfate; PTH, phenylthiohydantoin.

0006-2960/81/0420-5239$01.25/0